NEOPLASIA
www.neoplasia.com

Volume 22 Number 12 December 2020 pp. 689–701

Original Research

Niche-derived soluble DLK1 promotes glioma growth ☆,☆☆,★

Elisa S. Grassi[1]; Pauline Jeannot; Vasiliki Pantazopoulou; Tracy J. Berg; Alexander Pietras*

Division of Translational Cancer Research, Department of Laboratory Medicine, Lund University, Lund, Sweden

Abstract

Tumor cell behaviors associated with aggressive tumor growth such as proliferation, therapeutic resistance, and stem cell characteristics are regulated in part by soluble factors derived from the tumor microenvironment. Tumor-associated astrocytes represent a major component of the glioma tumor microenvironment, and astrocytes have an active role in maintenance of normal neural stem cells in the stem cell niche, in part via secretion of soluble delta-like noncanonical Notch ligand 1 (DLK1). We found that astrocytes, when exposed to stresses of the tumor microenvironment such as hypoxia or ionizing radiation, increased secretion of soluble DLK1. Tumor-associated astrocytes in a glioma mouse model expressed DLK1 in perinecrotic and perivascular tumor areas. Glioma cells exposed to recombinant DLK1 displayed increased proliferation, enhanced self-renewal and colony formation abilities, and increased levels of stem cell marker genes. Mechanistically, DLK1-mediated effects on glioma cells involved increased and prolonged stabilization of hypoxia-inducible factor 2alpha, and inhibition of hypoxia-inducible factor 2alpha activity abolished effects of DLK1 in hypoxia. Forced expression of soluble DLK1 resulted in more aggressive tumor growth and shortened survival in a genetically engineered mouse model of glioma. Together, our data support DLK1 as a soluble mediator of glioma aggressiveness derived from the tumor microenvironment.

Neoplasia (2020) 22, 689–701

Keywords: DLK1, Hypoxia, HIF-2a, Glioma, Tumor-associated astrocytes, Stem cell niche

* Corresponding author.
E-mail address: alexander.pietras@med.lu.se (A. Pietras).

☆ *Abbreviations:* ACM, astrocyte-conditioned media, CCGA, Chinese Glioma Genome Atlas, DLK1, delta like noncanonical Notch ligand 1, GBM, glioblastoma multiforme, GFAP, glial fibrillary acidic protein, HIF, hypoxia-inducible factor, HREs, hypoxia-responsive elements, IR, ionizing radiation, OCT, optimal cutting temperature compound, PDGF, platelet-derived growth factor, PFA, paraformaldehyde, PIGPC, Pdgfb-induced glioma primary culture, RCAS, replication-competent avian sarcoma-leukosis virus long-terminal repeat (LTR) with splice acceptor, RIPA, radioimmunoprecipitation assay, SVZ, subventricular zone, TCGA, The Cancer Genome Atlas.

☆☆ Funding: This work was supported by grants to AP from the Ragnar Söderberg Foundation (M20_16), the Swedish Cancer Society (19 0283; CAN 2016/328; CAN 2017/975), the Swedish Research Council (2014-02406; 2018-02864), the Swedish Childhood Cancer Fund (PR2017-0040; PR2014-0157; TJ2014-0016), Ollie & Elof Ericssons foundation, Jeanssons stiftelser, the Crafoord foundation, Gösta Miltons donationsfond, and Stiftelsen Cancera.

★ Declaration of Competing Interest: The authors declare no conflicts of interest.

[1] Present address: Department of Clinical Sciences and Community Health (DISCCO), University of Milan, Milan, Italy.

Social media: @pietraslab (A. Pietras)

Received 21 August 2020; received in revised form 30 September 2020; accepted 4 October 2020; Available online xxx

https://doi.org/10.1016/j.neo.2020.10.005

Introduction

Glioblastoma recurrence following standard-of-care treatment with radiotherapy, surgery, and chemotherapy invariably gives rise to incurable lesions, and the median survival following diagnosis remains at 12 to 20 months despite recent advances in our understanding of glioblastoma at a molecular level [1]. Evidence from human patient samples and murine models of brain tumors suggest that inherent therapeutic resistance within a subset of tumor cells with stem cell characteristics may be the primary source of recurrent tumors [2,3]. While the origin and fate of such cells remain controversial, glioblastoma cell phenotypes are highly plastic, and non−stem-like cells can acquire characteristics of stem cells as a result of microenvironmental interactions with the extracellular matrix, with growth factors, or as a result of altered oxygenation or pH [3–6]. Indeed, tumor cells with stem cell properties appear to be spatially restricted to specific microenvironments such as the perinecrotic and perivascular niches, suggesting that these niches may control residing tumor cell phenotypes [4,5,7].

Delta Like noncanonical Notch ligand 1 (DLK1) is a transmembrane protein in the Notch family of ligands, that is capable of signaling in a Notch-dependent and -independent manner depending on cellular context

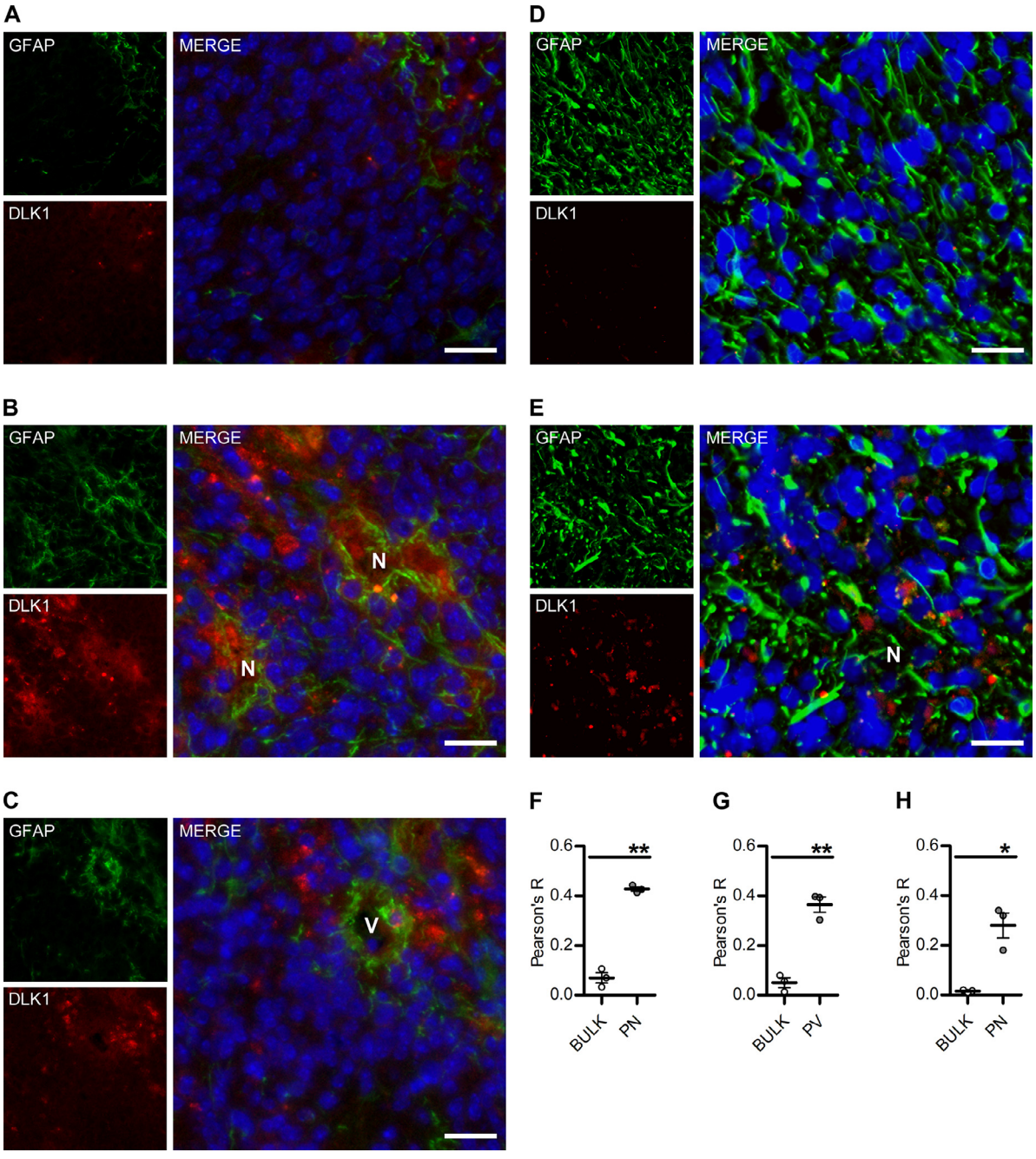

Figure 1. DLK1 expression in murine glioma. (A-C) Representative images of immunofluorescent stainings showing tumor-associated astrocytes and DLK1 localization in bulk tumor (A) and perinecrotic (N) and perivascular (V) areas (B, D, respectively) of shp53-induced murine gliomas. Scalebars represent 25 µm. (D, E) Representative images of immunofluorescent stainings showing tumor-associated astrocytes and N-terminal, secreted, DLK1 localization in bulk tumor (D) and perinecrotic areas (N) (E) of shp53-induced murine gliomas. (F-G) Colocalization analysis of immunofluorescent staining showing DLK1 and GFAP expression in bulk tumor vs perinecrotic (F) and perivascular (G) niches. (H) Colocalization analysis of immunofluorescent staining showing secreted DLK1 and GFAP expression in bulk tumor vs perinecrotic niche. Scalebars represent 25 µm. Statistical analysis: (A-H) $n = 3$. Statistical significance was determined with t test with Welch's correction for unequal variances applied to Pearson's coefficients (F-H). In the whole figure significance is represented as $^{*}P < 0.05$ and $^{**}P < 0.01$ vs bulk tumor. DLK1, delta-like noncanonical Notch ligand 1; GFAP, glial fibrillary acidic protein.

[8–13]. Expression of DLK1 is increased with tumor grade in glioma, and its signaling has been associated with various properties of aggressive tumor cells [14,15]. The mechanisms underlying these effects on tumor cell behavior remain poorly understood, but likely include signaling from the extracellular, soluble domain of DLK1 [16]. Indeed, soluble DLK1 secreted from astrocytes was recently shown to be a critical component of the subventricular zone neural stem cell niche [11]. Astrocytes represent a prominent cell type in the brain tumor microenvironment [17], and recent studies revealed that DLK1 is one of the top upregulated genes in tumor-associated astrocytes of high-grade vs low-grade gliomas [18]. The regulation of DLK1 expression is poorly

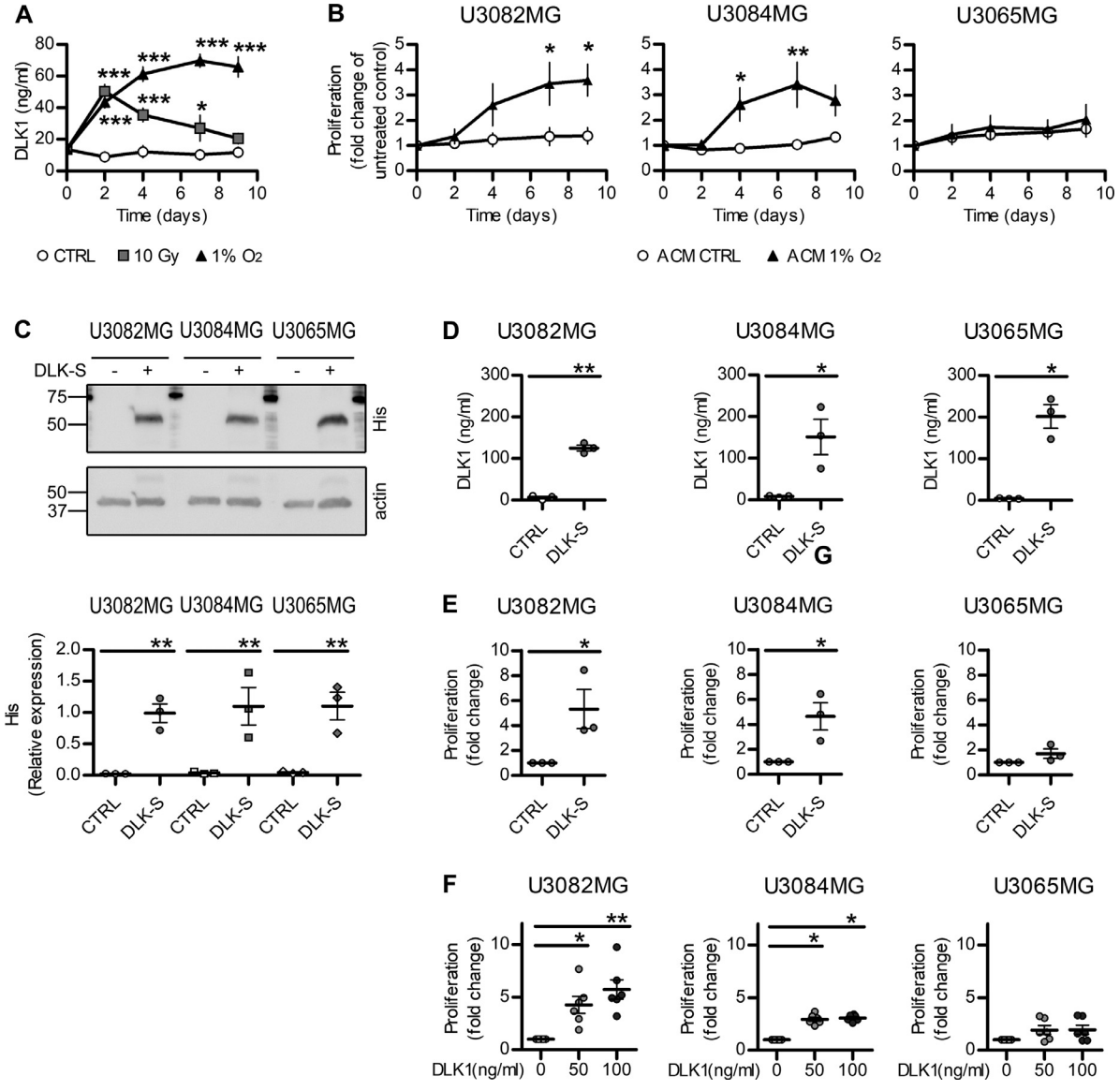

Figure 2. Effects of soluble DLK1 and astrocyte-derived factors on glioma cells. (A) ELISA assay data showing DLK1 secretion in human fetal astrocytes exposed to 1-time 10 Gy irradiation or 1% O_2 for up to 9 days. (B) Media transfer experiments showing the effects of normoxic and hypoxic Astrocyte-Conditioned media (ACM) on human glioma cell lines. (C) Representative images and densitometric analysis of western blots showing His-tagged soluble DLK1 expression in U3082MG, U3084, and U3065 cells transient transfection. (D) ELISA assay data showing DLK1 secretion in human glioblastoma cells transfected with soluble DLK1. (E) Media transfer experiments showing the effects of media from glioblastoma cells overexpressing soluble DLK1 on human glioma cell lines themselves. F: Proliferation assays of glioma cells treated with recombinant DLK1 for 72 hours. Statistical analysis: (A, B) $n = 4$ (C, D, E) $n = 3$, (F) $n = 6$. Statistical significance was determined by 2-way ANOVA (A, B) and t test (C-F), in E and F Welch's correction for unequal variances was applied. In the whole figure significance is represented as $^{*}P < 0.05$, $^{**}P < 0.01$, and $^{***}P < 0.001$ vs untreated controls. DLK1, delta-like noncanonical Notch ligand 1.

understood, but some elements of the brain tumor microenvironment such as hypoxia have been shown to drive DLK1 expression [19,20].

Here, we sought to investigate the role of soluble DLK1 in the high-grade glioma tumor microenvironment. We found increased secretion of DLK1 from tumor-associated astrocytes subjected to stresses of the tumor microenvironment, such as hypoxia and ionizing radiation. Soluble DLK1 increased proliferation and stem cell characteristics of glioma cells, and promoted tumor growth in a genetically engineered mouse model of glioma. Together, our findings suggest that soluble DLK1 is a niche-derived mediator of aggressive tumor growth in brain tumors.

Materials and methods

Glioma mouse models

Nestin-tv-a Ink4a/Arf$^{-/-}$ mice (IMSR Cat# NCIMR:01XH4, RRID:IMSR_NCIMR:01XH4) were intracranially injected with DF1 cells (ATCC Cat# CRL-12203, RRID:CVCL_0570) expressing replication-competent avian sarcoma-leukosis virus long-terminal repeat with splice acceptor (RCAS) encoding human platelet-derived growth factor B (PDGFB) and RCAS-short hairpin p53 (RCAS-shp53), as indicated, in the neonatal

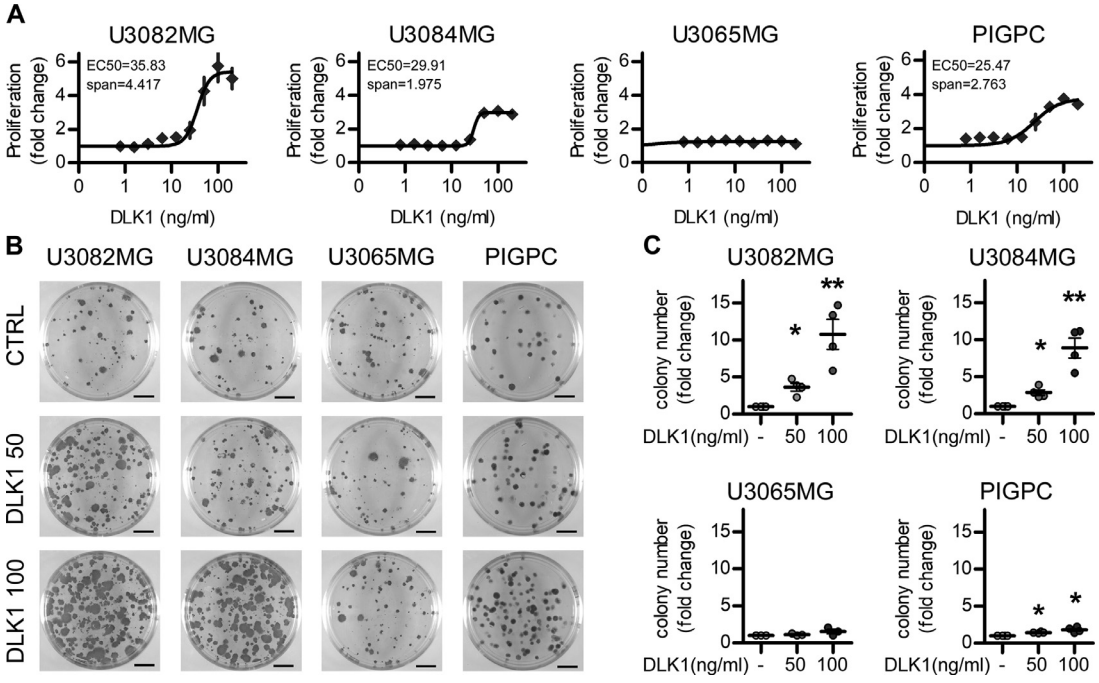

Figure 3. Effects of soluble DLK1 on glioma cells. (A) Proliferation curves of U3082MG, U3084MG, U3065MG, and PIGPC cells grown at increasing concentrations of recombinant DLK1 for 72 hours. Data are expressed as fold change of untreated control. (B, C) Representative images and quantification of colony forming ability of U3082MG, U3084MG, U3065MG, and PIGPC cells grown at increasing concentrations of recombinant DLK1. Data are expressed as fold change of untreated control. Statistical analysis: independent experimental replicates are as follow, (A) $n = 6$, except U3065MG where $n = 4$, (C) $n = 4$, Statistical significance was determined by 1-way ANOVA, followed by Bonferroni post hoc test. In the whole figure significance is represented as $^{*}P < 0.05$ and $^{**}P < 0.01$ vs untreated controls. DLK1, delta-like noncanonical Notch ligand 1; PIGPC, primary murine glioma cell.

brain with a 10-μL gas-tight Hamilton syringe, as described previously [21,22].

Soluble DLK-S was cloned into the RCAS vector and mice were co-injected with a 1:1 mix of DF1 cells expressing RCAS-PDGFB and RCAS-DLK-S or empty RCAS as indicated. Each litter was allocated to 1 experimental group. Mice were monitored daily and sacrificed upon displaying brain tumor symptoms. All procedures were approved by the Swedish Board of Agriculture through the Malmö-Lund Regional Committee (permit M186–14). The sample number was determined based on the law of diminishing returns with the resource equation method (total number of animals - total number of groups >10). A total of 6 pups were excluded due to nontumor symptoms during week 0 to 3, the final numbers were $n = 26$ for PDGFB and $n = 24$ for DLK-S.

Immunofluorescence

Whole brains were embedded in optimal cutting temperature compound (OCT) (ThermoFisher) and frozen in precooled isopentane. Five micrometers thick cryosections were air-dried for 30 minutes, then fixed in ice-cold acetone or 4% paraformaldehyde and permeabilized using 0.3% Triton X-100 in phosphate buffered saline (PBS) (Sigma). Blocking was performed using serum-free protein block (DAKO), then sections were incubated overnight with primary antibodies at 4 °C with background reducing components (DAKO). Alexa Fluor secondary antibodies (Abcam) were used, and Vectashield Mounting medium with DAPI (Vector Laboratories) was used for mounting.

Primary antibodies: Pref-1/DLK1/FA1 antibody (Novus, Cat# NBP2-33697), DLK1 polyclonal antibody (Thermo Fisher Scientific Cat# PA5–72199, RRID:AB_2718,053), Mouse Pref-1/DLK1/FA1 Antibody (R and D Systems, Cat# AF8277), hypoxia-inducible factor 2 alpha (HIF-2a) antibody (Abcam Cat# ab199, RRID:AB_302739), Goat Anti-Human Olig2 (R and D Systems Cat# AF2418, RRID:AB_2157554), Chicken Anti-GFAP (Abcam Cat# ab4674, RRID:AB_304558), Ki-67 antibody (Thermo Fisher Scientific Cat# RM-9106-S0, RRID:AB_2341197).

Secondary antibodies: Donkey Anti-Goat IgG H&L Alexa Fluor 555 (Abcam Cat# ab150134, RRID:AB_2715537), Donkey anti-Rabbit IgG ($H + L$) Alexa Fluor 488 (Thermo Fisher Scientific Cat# A-21206, RRID:AB_2535792), Donkey anti-Chicken IgY H&L FITC (Abcam Cat# ab63507, RRID:AB_1139472) Goat anti-Rabbit IgG ($H + L$) Alexa Fluor 568 (Thermo Fisher Scientific Cat# A-11011, RRID:AB_143157).

Images were acquired using an Olympus BX63 microscope and DP80 camera and CellSens software (Olympus CellSens Software, RRID:SCR_016238).

For DLK1 and GFAP localization images (Figure 1), minimal postproduction consisting of background subtraction and automated level optimization was equally applied with ImageJ (Fiji, RRID:SCR_002285).

Colocalization analysis was performed with ImageJ (Fiji, RRID:SCR_002285) Coloc2 plugin on the selected Regions of Interest of at least 3 independent experiments.

Ki67 quantification was performed with CellProfiler (CellProfiler Image Analysis Software, RRID:SCR_007358), at least 3 fields were analyzed for each tumor, for a total of 101,717 nuclei analyzed, with $n = 45{,}466$ for PDGFB tumors and $n = 56{,}251$ for DLK-S tumors.

Areas of necrosis were identified by 2 independent researchers based on cellularity and the presence of pseudopalisading nuclei, based on the DAPI stain. Vessels were identified by morphological inspection of DAPI and GFAP stains.

Cell culture and treatments

Primary murine glioma cells (PIGPCs [23]) were cultured as described in DMEM (Life Technologies) + 10% fetal bovine serum and 1%

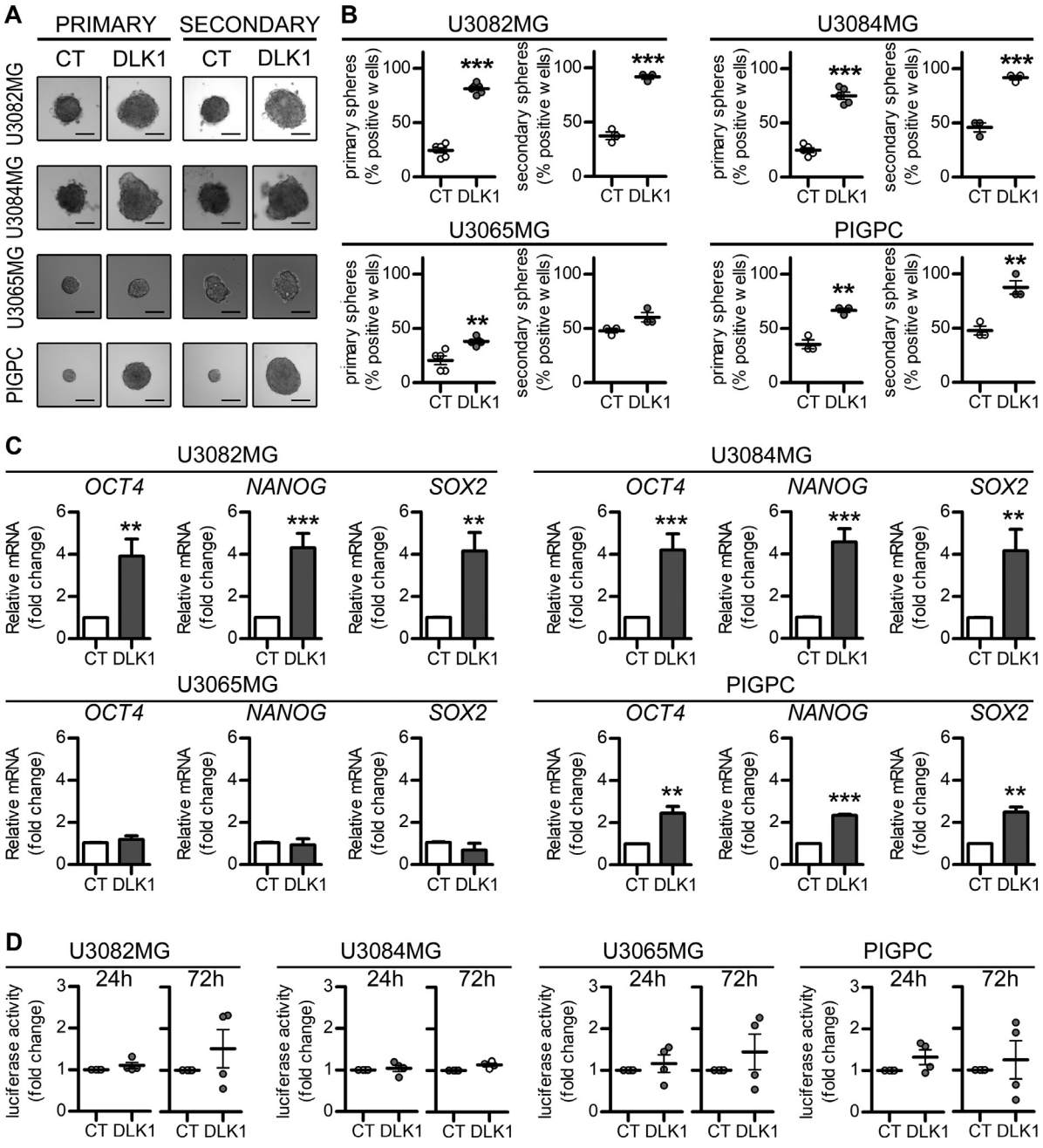

Figure 4. Effects of soluble DLK1 on glioma cell stem cell characteristics. (A, B) Representative images and quantification of primary and secondary sphere forming assays in U3082MG, U3084MG, U3065MG, and PIGPC cells grown at 0 or 50 ng/ml recombinant DLK1. (C) qPCR data for relative mRNA expression of *OCT4, NANOG,* and *SOX2* in U3082MG, U3084MG, U3065MG, and PIGPC cells grown at 0 or 50 ng/mL recombinant DLK1 for 72 hours. Data are expressed as fold change of untreated control. (D) 8xCSL-luciferase experiments showing Notch activity in cell lines untreated or treated with 50 ng/mL recombinant DLK1 for 24 and 72 hours. Results are expressed as fold change of respective controls. Statistical analysis: independent experimental replicates are as follow, (B) $n = 5$ for U3082MG, U3084MG, and U3065MG primary spheres and $n = 3$ PIGPC cells, (C) $n = 8$ except PIGPC where $n = 3$, (D) $n = 4$. Statistical significance was determined by t test, in C and D Welch's correction for unequal variances was applied. In the whole figure significance is represented as $^{*}P < 0.05$, $^{**}P < 0.01$, and $^{***}P < 0.001$ vs untreated controls. DLK1, delta-like noncanonical Notch ligand 1; PIGPC, primary murine glioma cell.

PenStrep (Corning). U3082MG (RRID:CVCL_IR93), U3084MG (RRID:CVCL_IR94) and U3065MG (RRID:CVCL_IR87) cells were from a human glioblastoma cell culture resource and were cultured as described [24] in Neurobasal medium (GIBCO)/DMEM/F12 with Glutamax (Life Technologies) +1% PenStrep solution, N2 and B27 (Life Technologies), 10 ng/mL epidermal growth factor, and 10 ng/mL fibroblast growth factor (Peprotech). Cells were dissociated using Accutase (ThermoFisher), and cultured as monolayers in dishes coated with polyornithine (Sigma) and laminin (Biolamina). Primary Human Astrocytes (3H Biomedical Cat# 1800-10) were cultured in Human Astrocyte Medium #SC1801 (3H Biomedical) and were used below passage 15. A Gamma Cell-3000 Elan (MDS Nordion) was used to deliver 10 Gy in a single dose. A Whitney

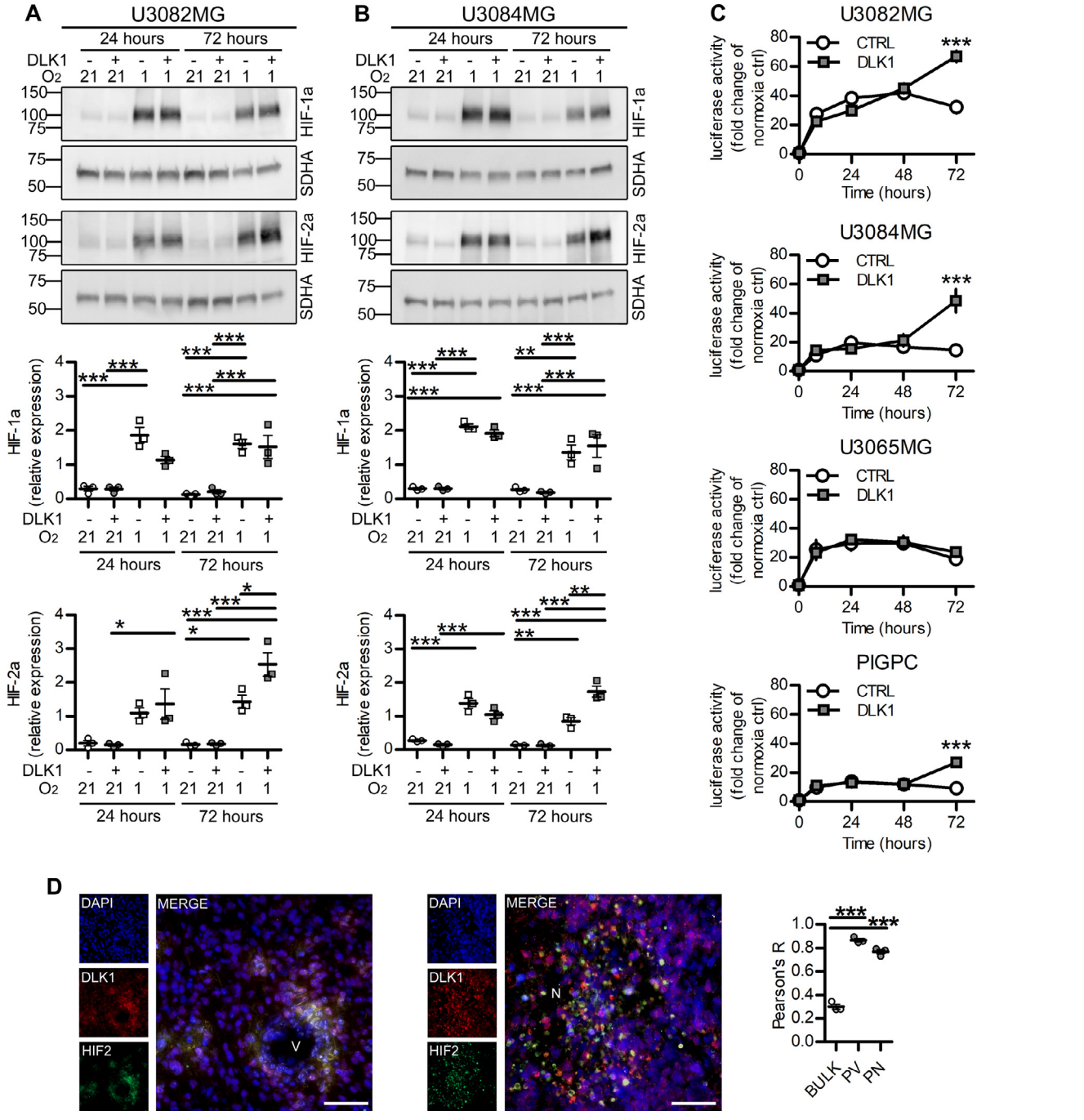

Figure 5. Effects of soluble DLK1 on HIF-2alpha activity under hypoxia. (A) Representative images and densitometric analysis of western blots showing HIF-1alpha (HIF-1a) and HIF-2alpha (HIF-2a) expression in U3082MG cells after treatment with 50 ng/mL recombinant DLK1 or hypoxia exposure as indicated in the figure. (B) Representative images and densitometric analysis of western blots showing HIF-1alpha (HIF-1a) and HIF-2alpha (HIF-2a) expression in U3084MG cells after treatment with 50 ng/mL recombinant DLK1 or hypoxia exposure as indicated in the figure. (C) HRE-luciferase time course experiments showing hypoxia response in cell lines untreated or treated with 50 ng/mL recombinant DLK1 and grown in 1% O_2 for up to 72 hours. Results are expressed as fold changes of respective normoxic controls. (D) Representative images and colocalization analysis of immunofluorescent staining showing DLK1 and HIF2-alpha (HIF2) expression in perivascular and hypoxic niches. Scale bars represent 50 µm. Statistical analysis: independent experimental replicates are as follow, (A, B) $n = 3$, (C) $n = 5$ for U3082MG and $n = 4$ for the other cell lines, (D) $n = 3$. Statistical significance was determined by 1-way ANOVA (A, B) followed by Bonferroni post hoc test, 2-way ANOVA (C), 1-way ANOVA of Pearson's coefficients (D). In the whole figure significance is represented as $^{*}P < 0.05$, $^{**}P < 0.01$, and $^{***}P < 0.001$ vs control or as indicated by straight lines. DLK1, delta-like noncanonical Notch ligand 1; HIF, hypoxia-inducible factor; HRE, hypoxia-responsive element; N, necrosis; V, vessel.

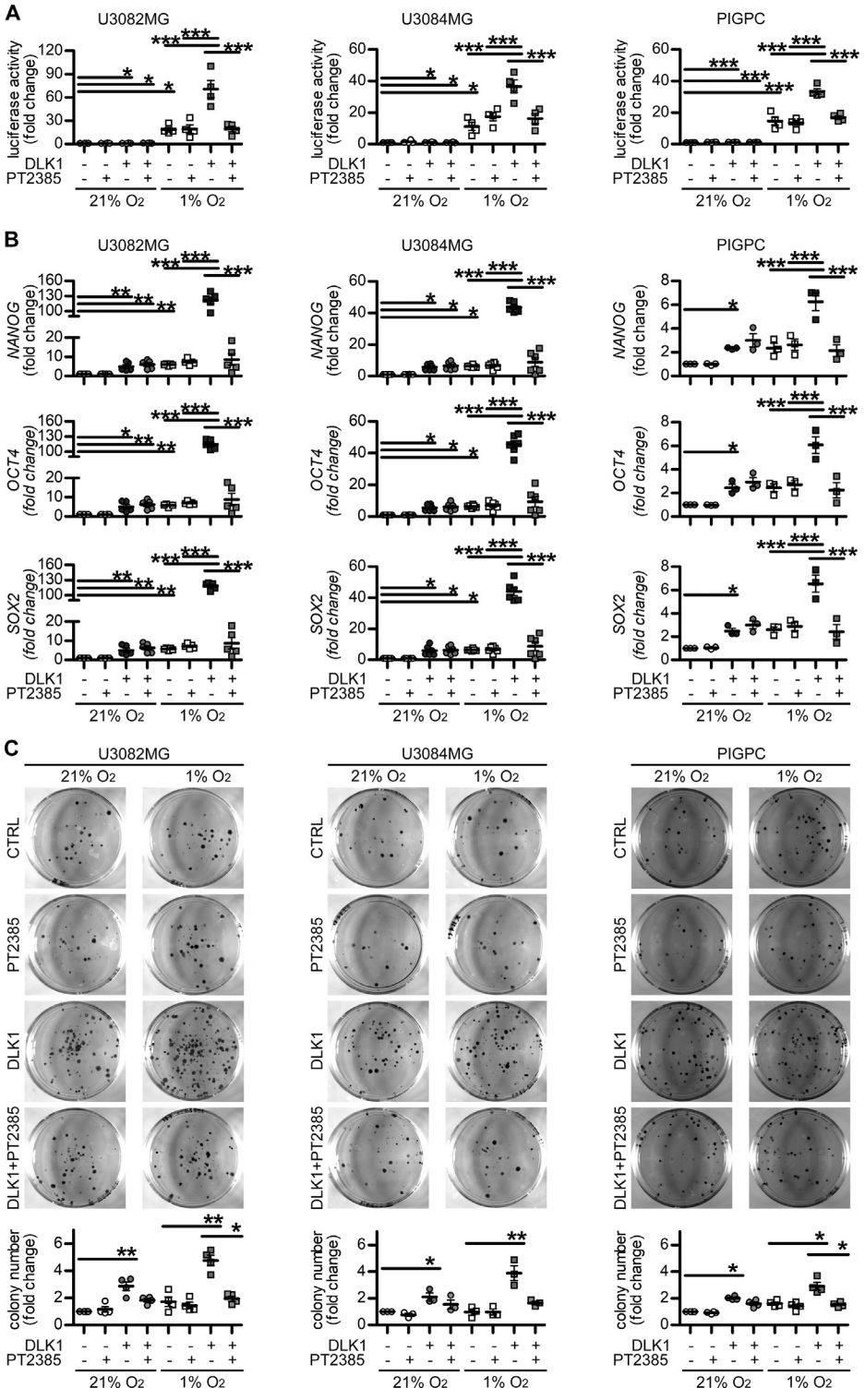

Figure 6. Effects of HIF-2alpha inhibition on DLK1-mediated effects under hypoxia. (A) HRE-luciferase experiments showing hypoxia response in cell lines untreated or treated with 50 ng/mL recombinant DLK1, 10 μM PT2385 and grown in 21% or 1% O_2 for 72 hours. Results are expressed as fold changes of respective normoxic controls. (B) qPCR data for relative mRNA expression of *NANOG, OCT4,* and *SOX2* in U3082MG, U3084MG and PIGPC cells pretreated with 50 ng/mL recombinant DLK1, 10 μM PT2385 and exposed to hypoxia for 72 hours as indicated in the figure. Data are expressed as fold change of untreated normoxic control. (C) Representative images and quantification of colony forming ability of U3082MG, U3084MG and PIGPC cells pretreated with 50 ng/mL recombinant DLK1, 10 μM PT2385 and exposed to hypoxia as indicated in the figure. Data are expressed as fold change of untreated normoxic control. Statistical analysis: independent experimental replicates are as follow, (A) $n = 4$, (B) $n = 6$ for U3082MG and U3084MG and $n = 3$ for PIGPC, (C) $n = 4$. All data are expressed as mean ± SEM. Statistical significance was determined by 1-way ANOVA followed by Bonferroni post hoc test. In the whole figure significance is represented as $^{*}P < 0.05$, $^{**}P < 0.01$, and $^{***}P < 0.001$ as indicated by straight lines. DLK1, delta-like noncanonical Notch ligand 1; HIF, hypoxia-inducible factor; HRE, hypoxia-responsive element; PIGPC, primary murine glioma cell.

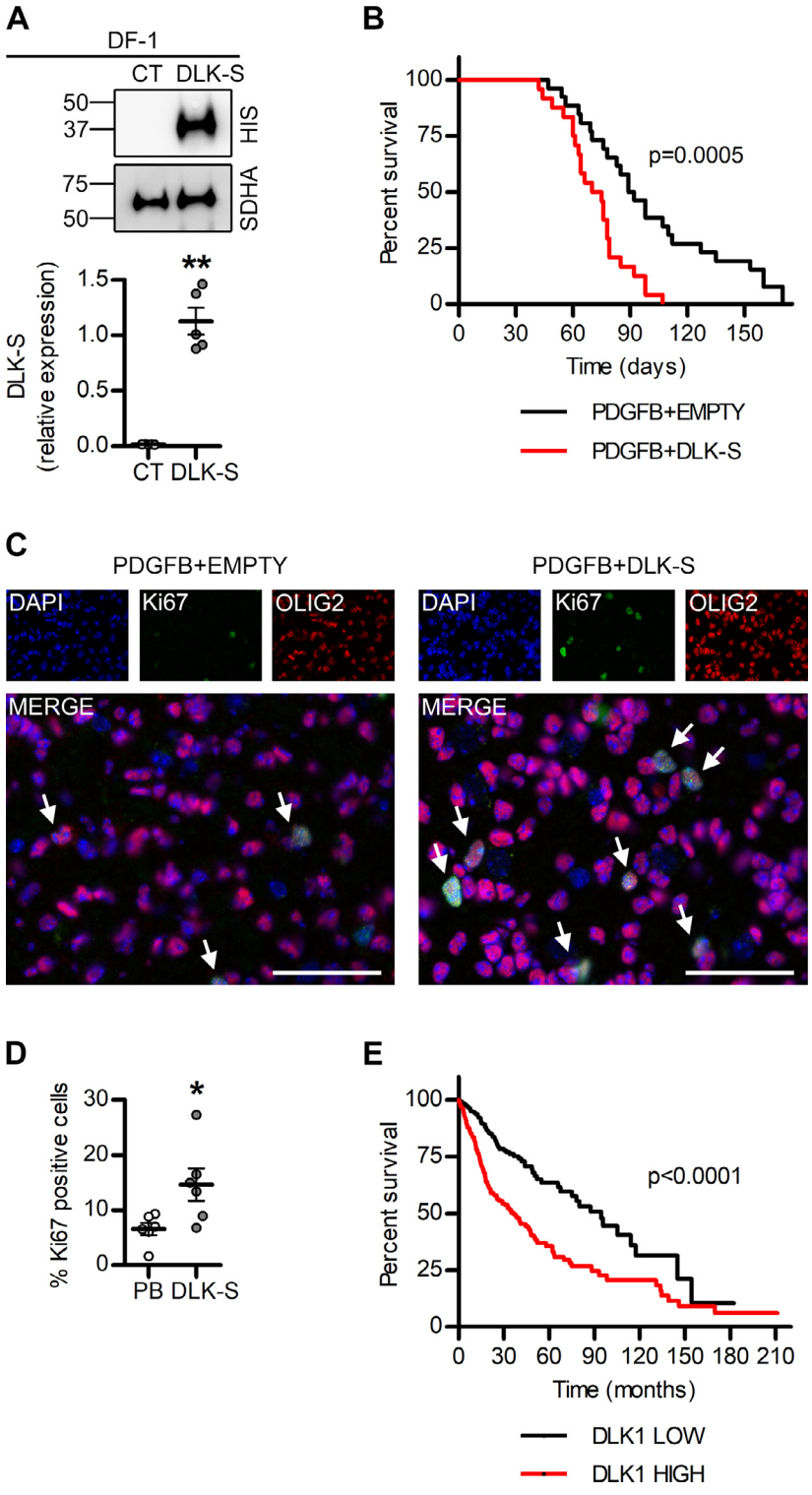

Figure 7. Effects of soluble DLK1 on glioma growth in vivo. (A) Representative images and densitometric analysis of western blots showing HIS-tagged DLK-S expression in DF1 cells transfected with empty or DLK-S RCAS vectors. (B) Kaplan-Meier survival plot of PDGFB-induced tumors with (DLK-S, red line) or without (EMPTY, black line) DLK1 overexpression. (C, D) Representative images and quantification of immunofluorescent stainings showing Ki67 positive cells expressed as percentage of tumor cells identified by OLIG2 staining. Scalebars represents 50 µm. (E) Kaplan-Meier survival plot of DLK1-HIGH (red line) and DLK1-LOW (black line) patients in TCGA GBMLGG data set. Statistical analysis: independent experimental replicates are as follow, (A) $n = 4$, (B) $n = 21$ for PDGFB and $n = 27$ for DLK-S, (C) $n = 6$, E $n = 333$, events = 82 for DLK1-low and $n = 334$, events = 157 for DLK1-high. Statistical significance was determined by t test with Welch's correction (A), Kaplan-Meier survival plot with log-rank Mantel-Cox test (B, C) and Mann-Whitney (D). In the whole figure significance is represented as $^{*}P < 0.05$, $^{**}P < 0.01$ vs control. DLK1, delta-like noncanonical Notch ligand 1; DLK-S, soluble part of DLK1; PDGFB, platelet-derived growth factor B; RCAS, replication-competent avian sarcoma-leukosis virus long-terminal repeat (LTR) with splice acceptor; TCGA, The Cancer Genome Atlas. (Color version is available online.)

H35 Hypoxystation (Don Whitley Scientific) was used to generate hypoxic conditions.

Cells were treated with the indicated concentrations of DLK1 human (Sigma Cat# SRP8006) or Recombinant Human DLK-1 protein (Abcam Cat# ab151926). For HIF-2a inhibition, cells were treated with 10 μM PT2385 (MedChemExpress Cat# HY-12867) or equivalent amount of DMSO 24 hours prior hypoxia exposure and kept in the dark for the whole experiment. Transient transfection was performed with X-tremeGENE 9 DNA Transfection Reagent (Sigma Cat# 06 365 809 001) following manufacturer's recommendations. Human DLK1 ectodomain expression vector was obtained from Addgene (DLK1-bio-His, RRID:Addgene_51876) [25].

DLK1 ELISA assay

DLK1 secretion was measured with Human Pref-1 enzyme-linked immunosorbent assay (ELISA) kit for cell culture supernatants, plasma and serum samples RAB 1076 (Sigma-Aldrich). Medium from control and treated astrocytes was collected every 2 to 3 days while medium from DLK-S transfected cells was collected 72 hours hours post transfection, immediately snap frozen in dry ice and stored at −80 °C until the day of the assay. The enzyme-linked immunosorbent assay (ELISA) was performed following manufacturer's instructions and 450 nm absorbance was read on a Synergy 2 plate reader (BioTek).

Proliferation assay

Thousand cells/well (PIGPC) or 2500 cells/well (U3082MG, U3084MG and U3065MG) were seeded in 96 well plates. For astrocyte conditioned media (ACM) transfer experiments, 24 hours after seeding, media from Astrocyte and transfected cells was filter sterilized and used to replace culture media. For astrocyte experiments, media was replaced every 2 to 3 days and proliferation was assessed after 9 days. For transfected cells, proliferation was assessed after 72 hours.

For recombinant protein experiments, 24 hours after seeding cells were treated with serial dilutions of recombinant DLK1 (0–200 ng/mL range) and grown for 72 hours. At the moment of the assay, 10 μL of WST-1 solution (Roche) were added to each well and after 2 hours of incubation at 37 °C and 5% CO2 450 nm absorbance was read on a Synergy 2 plate reader (BioTek).

Western blot

Cells were lysed in radioimmunoprecipitation assay buffer supplemented with Complete Phosphatase and Complete Protease inhibitor cocktails (Roche). After dilution in Laemmli buffer with DTT and boiled for 5 minutes, samples were loaded on 4% to 20% Mini-PROTEAN TGX Precast Protein Gels (Biorad). Proteins were transferred on polyvinylidene fluoride (PVDF) membranes using a Transblot Turbo System (Biorad), blocked in 5% nonfat dry milk/PBS, and incubated overnight at 4 °C with primary antibodies. After washing, membranes were incubated for 1 hour with secondary antibodies (Abcam). Images were acquired using a Fujifilm LAS 3000 Imager. Densitometric analysis were performed with ImageJ software (Fiji, RRID:SCR_002285). Band signal intensity was normalized for the respective loading control values (actin or SDHA).

Primary antibodies: hypoxia-inducible factor 1 alpha HIF-1a antibody (Novus Cat# NB100-479SS, RRID:AB_790147), HIF-2a antibody (Abcam Cat# ab199, RRID:AB_302739), SDHA antibody (Abcam Cat# ab14715, RRID:AB_301433), 6X His-tag antibody (Abcam Cat# ab9108, RRID:AB_307016), beta Actin antibody (Abcam Cat# ab75186, RRID:AB_1280759). Secondary antibodies: Goat anti-Rabbit IgG (*H* + *L*) Secondary Antibody, HRP (Thermo Fisher Scientific Cat# 31460, RRID:AB_228341), Goat anti-Mouse IgG (*H* + *L*) Secondary Antibody, HRP (Thermo Fisher Scientific Cat# 31430, RRID:AB_228307).

Colony and sphere formation assays

Mechanical dissociation with Accutase (ThermoFisher) was used to prepare single cell suspensions. Cells were counted using a hemocytometer. For colony formation assay, 350 cells were seeded in 5 cm dishes coated with polyornithine (Sigma) and laminin (Biolamina). U3082MG, U3084MG and U3065MG cells were cultured for 14 days while PIGPCs for 8 days, under the indicated conditions, then washed in PBS and fixed using 4% paraformaldehyde. Cells were stained using 0,01% crystal violet/H2O. Wells were washed gently in water, then air-dried for 24 hours. Images were acquired with a Fujifilm LAS 3000 Imager.

Sphere formation assay was performed with the hanging-drop method. 10 cells in 35 μL drops were seeded on the lid of a 48 well plate and grown under the indicated conditions for 2 weeks. For secondary sphere assay, primary spheres were pooled, pelleted, dissociated with Accutase and reseeded at the indicated conditions. Wells with spheres were manually counted and images were acquired with a Zeiss AX10 inverted microscope.

Real-time quantitative PCR

The RNeasy Mini Kit was used with Qiashredder (QIAGEN) according to the manufacturer's instructions for RNA isolation, and cDNA was synthesized using random primers and Multiscribe reverse transcriptase (Applied Biosystems). A QuantStudio 7 real-time PCR system (Applied Biosystems) with SYBR Green Master Mix (Applied Biosystems) was used for amplification. Gene expression levels were normalized to the expression of 3 housekeeping genes (UBC, SDHA, and YWHAZ) using the comparative ΔΔCT method.

The following primers were used: *NANOG* (GCTGGTTGCCTCA TGTTATTATGC; CCATGGAGGAAGGAAGAGGAGAGA), *SOX2* (GC CTGGGCGCCGAGTGGA; GGGCGAGCCGTTCATGTAGGTCTG), *OCT4* (GCCTGGGCGCCGAGTGGA; CCACATCGGCCTGTGTATA TC), *UBC* (ATTTGGGTCGCGGTTCTT; TGCCTTGACATTCTCG ATGGT), *SDHA* (TGGGAACAAGAGGGCATCTG; CCACCACTGC ATCAAATTCATG), *YWHAZ* (ACTTTTGGTACATTGTGGCTTCAA; CCGCCAGGACAAACCAGTAT)

Transfections and luciferase reporter assay

DLK-S expression plasmid was kindly provided by prof. Anne Ferguson-Smith [11], cloned into RCAS vector by classic restriction enzyme technique and transfected into DF-1 cells. For luciferase reporter assay, cells were co-transfected with hypoxia-responsive element (HRE)-luc (Addgene) [26] or 8xCSL-luc (gift from Håkan Axelson) and pCMV-renilla (Promega) and analyzed using the Dual-Luciferase Reporter Assay System (Promega) on a Synergy 2 platereader (BioTek). Xtreme gene 9 (Roche) reagent was used according to manufacturer's recommendations for transient transfections.

Statistical analyses

For DLK1 expression and patients survival, data from 620 patients from The Cancer Genome Atlas (TCGA, RRID:SCR_003193, https://portal.gdc.cancer.gov/) [27] and the Chinese Glioma Genome Atlas [28], were analyzed using GlioVis ((http://gliovis.bioinfo.cnio.es/) [29]) (DLK1-LOW $n = 333$, events = 82, median = 87.5; DLK1-HIGH $n = 334$, events = 157, median = 34.9).

For proliferation experiments, the EC50 and span were estimated with a nonlinear regression curve, using a log. agonist vs normalized response (variable slope) equation fitted in Graphpad Prism 5 (GraphPad Prism, RRID:SCR_002798). For immunofluorescence experiments, colocalization was measure by Pearson's R coefficient in 3 independent experiments with ImageJ Coloc2 plugin. For Ki67 quantification, at least 3 fields were analyzed for each tumor, for a total of 101,717 nuclei analyzed, with $n = 45{,}466$ for PDGFB tumors and $n = 56{,}251$ for DLK-S tumors.

After normal distribution and variance similarity evaluation, 2-sided unpaired t test (eventual Welch's correction for groups with different variances), Mann-Whitney for nonparametric data, 1-way ANOVA with Bonferroni post hoc test and 2-way ANOVA (timelines only) tests were used to determine statistical significance, as indicated in respective figure legends. For survival evaluation, the Kaplan–Meier method was used to investigate variables and overall survival correlation, while a log-rank test was employed to compare survival curves. In all figures data are shown as mean±SEM, analyzed using GraphPad Prism 5 software and significance expressed as P values ($^{*}P < 0.05$, $^{**}P < 0.01$, $^{***}P < 0.001$).

Data availability

The data that support the findings of this study are available from the corresponding author upon reasonable request.

Results

DLK1 is expressed and secreted by tumor-associated astrocytes in the glioma microenvironment

To test whether tumor-associated astrocytes could be a source of DLK1 in the glioma tumor microenvironment, we generated PDGFB/shp53-induced murine gliomas using the RCAS/tv-a system as previously described [14], then co-stained tumors for the astrocyte marker glial fibrillary acidic protein (GFAP) and DLK1. While the bulk of the tumor cells appeared negative for DLK1 expression, DLK1 signal was detected in areas of GFAP staining both in perinecrotic and perivascular tumor areas, and both in GFAP positive and negative cells, suggesting DLK1 expression in astrocytes, tumor cells, and potentially other cell types present in these areas (Figure 1A−C, F−G and Supplementary Figure 1A−B).

The use of an independent antibody directed against the N-terminal, soluble domain of DLK1 also showed specific signal in the perinecrotic tumor areas (Supplementary Figure 2) and co-staining of GFAP and DLK1 (Figure 1D−E, H and Supplementary Figure 1C).

DLK1 gene expression was previously reported to be upregulated in isolated GFAP+ tumor-associated astrocytes of high-grade glioma compared to those of lower-grade tumors [18], further confirming DLK1 expression in astrocytes in this model system. We speculated that this DLK1 induction could be mediated by microenvironmental factors. As hypoxia is 1 major microenvironmental reality of high-grade glioma compared to low-grade glioma [5,30], we cultured human fetal astrocytes under normoxic or hypoxic conditions for up to 10 days. We also subjected astrocytes to a single dose of irradiation to mimic another physiological response to a therapeutic intervention relevant to high-grade glioma. Both astrocytes subjected to growth in hypoxia and those subjected to irradiation displayed increased DLK1 levels secreted into the culture media, as measured by an ELISA assay (Figure 2A). The higher levels of DLK1 in the media were sustained for the entire 10 day period in the case of astrocytes cultured in hypoxia, whereas irradiated astrocytes displayed a peak secretion at 2 days post-treatment with levels returning to baseline after 9 days (Figure 2A). Together, these data support that astrocytes may secrete DLK1 into the tumor microenvironment in glioma.

Soluble DLK1 promotes glioma cell proliferation, survival and self-renewal

We next examined what effect soluble DLK1 may have on glioma cells.

We first performed a media transfer experiment by treating human glioblastoma cell lines maintained in serum-free, stem cell-promoting conditions with media from astrocytes cultured in normoxic (ACM CTRL) and hypoxic (ACM 1% O_2) conditions for up to 9 days. In 2 out of 3 cell lines, media from hypoxic astrocytes induced a significant increase in the proliferation rate (Figure 2B). Since ACM contains many other different factors that may influence cancer cell growth, we then directly investigated the effects of soluble DLK1 with 2 different approaches. First, we transiently transfected human glioblastoma cell lines with a plasmid containing the N-terminal soluble part of DLK1 (DLK-S, His-tagged). All the 3 transfected cell lines overexpressed and secreted similar levels of DLK-S, as verified by western blot and ELISA experiments (Figure 2C−D). A media transfer experiment showed that 2 out of 3 cell lines significantly increased their proliferation (Figure 2E) when grown in DLK-S conditioned media. We then treated the human glioblastoma cell lines with a recombinant protein corresponding to the DLK1 secreted part, and once again, the 2 DLK-responding cell lines showed significant increase in their proliferation (Figure 2F). Taken together, these data demonstrate that soluble DLK1 is able to induce glioma cell proliferation, irrespectively of its origin.

As the use of the recombinant protein allows for better control of DLK1 concentrations, we then moved forward with this approach. We first generated a dose-response curve in all 3 human glioblastoma cell lines and in PDGFB-induced glioma primary cultures (PIGPCs) derived from the glioma mouse model. All the cell lines, with the exception of the nonresponding U3065MG, showed a dose dependent increase in cell proliferation, with a plateau obtained at 200 ng/mL DLK1 and EC50s in between 25 and 35 ng/mL (Fig 3A).

In line with these findings, all cell lines that responded to DLK1 in the proliferation assay also increased their colony formation ability in a dose-dependent manner when exposed to sub-maximal soluble DLK1 concentrations similar to those obtained in hypoxic astrocytes (Figure 3B−C).

Furthermore, soluble DLK1 strongly enhanced the self-renewal ability of responsive glioma cell lines, as measured by the serial sphere-formation assay (Figure 4A−B) performed at clonal density (Supplementary Figure 3), and induced a significant increase in the stem cell markers *OCT4, NANOG,* and *SOX2* (Figure 4C). Since DLK1 has been reported to influence the Notch pathway [8,12], we tested if these effects were Notch-dependent. Luciferase experiments performed at different time points revealed no significant alterations in Notch activity in any tested cell lines (Figure 4D).

DLK1-effects are mediated in part by HIF-2a

Because DLK1 secretion was increased by astrocytes under hypoxic conditions, and because of known previous links between DLK1 expression and function to hypoxia [20], we asked whether soluble DLK1 could influence the hypoxic response of glioma cells. We cultured U3082MG and U3084MG human glioblastoma cells for 24 or 72 hours in 1% O_2, stimulated or not with soluble DLK1. While there was no difference in HIF-1a stabilization with DLK1 treatment, Western blots showed significantly increased HIF-2a protein levels at 72 hours in cells cultured with soluble DLK1 (Figure 5A−B). This increased HIF-2a expression was reflected in a stronger hypoxic response, as 2/3 human glioblastoma lines and PIGPCs displayed increased activation of HREs at 72 hours of culture in hypoxia with DLK1 stimulation, as measured in an HRE-luciferase assay (Figure 5C). Moreover, analysis of PDGFB/shp53-induced murine gliomas revealed that both DLK1 and HIF-2a were strongly expressed and showed a significant co-localization only in the perivascular and perinecrotic niches (Fig. 5D).

As HIF-2a is a known driver of stem cell characteristics in glioma and other tumor forms [31,23,32–34], we next tested whether effects of DLK1 on glioma cell behavior were mediated by HIF-2a. The treatment with the specific HIF-2a inhibitor PT2385 at concentrations with significant effects on HIF-2a protein [35,36] (Supplementary Fig. 4) was able to revert the DLK1-induced increase in hypoxia response (Figure 6A). Similarly, while stimulation of glioma cells with soluble DLK1 boosted the increase in the expression of the stem cell marker genes *NANOG, OCT4,* and *SOX2* in hypoxic cells, addition of PT2385 blocked this specific DLK1 effect in all cell lines tested (Figure 6B). Moreover, PT2385 decreased the colony formation ability of glioma cells exposed to soluble DLK1 in hypoxia (Figure 6C). Notably however, PT2385 treatment did not significantly affect DLK1-induced gene expression in normoxia, and showed surprisingly modest effects in DLK1-untreated cells at hypoxia. Together, these data suggest that DLK1 promotes the glioma stem cell character in part via HIF-2a stabilization.

DLK1 promotes aggressive glioma growth in vivo

To test the effects of soluble DLK1 on glioma growth in vivo, we generated a mouse model for the overexpression of soluble DLK1 together with PDGFB using the RCAS/tv-a system (Figure 7A). Co-injection of RCAS-PDGFB with RCAS-DLK-S (soluble) resulted in more aggressive tumors as compared to RCAS-PDGFB with empty vector control, as measured by survival time following injections (Figure 7B). Evaluation of Ki67 expression revealed a significant increase in cell proliferation in murine DLK-S tumors as compared to controls (Figure 7C, D), thus confirming the in vitro data (Figure 2E–F, 3A). In agreement with our in vivo data using a mouse model that gives rise to a range of low-to-high-grade gliomas, analysis of the human TCGA LGGGBM data set [27] revealed that tumors expressing high levels of *DLK1* were significantly more aggressive than those with low levels of *DLK1* (Figure 7E), presumably as a result of the higher *DLK1* levels reported in high-grade glioma. These findings were replicated in an independent data set (Supplementary Figure 5A–B). Notably, in data sets comprising GBM only, *DLK1* expression was either associated with slightly longer survival, or not associated with any significant survival difference at all, suggesting that the link between *DLK1* and shorter survival in the LGGGBM data set is related to increased expression in higher-grade tumors (Supplementary Figure 5A–B).

Discussion

An increasing focus on cancer stem cell characteristics has revealed parallels between normal neural stem cell regulation and cancer stem cell characteristics in brain tumors [37,38]. Control over tumor cell phenotypes by specific, local microenvironments within a tumor, for example, is reminiscent of the way that normal tissue stem cells reside within and rely on their niche to maintain the stem cell character [3,4]. It is likely that some of the same mechanisms involved in neural stem cell maintenance in the vascular niche of the subventricular zone may also be involved in maintaining the cancer stem cell character of brain tumor cells located in a perivascular or periarteriolar [39] niche. We describe one such example here: soluble DLK1 secreted from astrocytes appears to be involved in stem cell maintenance both of normal neural stem cells and glioma cells, as shown here. An association between DLK1 expression and aggressive tumor growth in glioblastoma has previously been established [20]. By generating a mouse model for testing effects of soluble DLK1 overexpression specifically in the context of glioblastoma, we show that the previously reported association between DLK1 expression and tumor grade in glioma [14,15] may at least in part be caused by DLK1 itself, as soluble DLK1-overexpressing tumors had a higher proliferation rate and significantly decreased mice survival as compared to controls. It is important to note that DLK1 expression is not limited to tumor-associated astrocytes, and soluble DLK1 may be derived both from other stromal cell types and tumor cells themselves. Our experiments indicate that soluble DLK1 affects tumor cell proliferation similarly regardless of whether it was produced by astrocytes or tumor cells. In a previous study, we described release of and signaling from the intracellular domain of DLK1 in glioma cells [14]. Data presented here do not link signaling from the soluble DLK1 to that of the intracellular fragment, however, both appear to be regulated by the hypoxic tumor microenvironment. It is yet unclear whether or not DLK1 expression is required in tumor cells to be affected by soluble DLK1 secreted into the niche [11].

As with astrocyte-derived DLK1 in regulation of normal neural stem cells, the exact mechanism(s) by which soluble DLK1 signals to glioma cells remains to be investigated. We show here that soluble DLK1 can contribute to a stronger and more prolonged response to hypoxia, as mediated by increased HIF-2a stabilization in DLK1 treated cells. This effect on HIF-2a stabilization indeed seemed important for the tumor-promoting effects of DLK1 signaling as inhibition of HIF-2a transcriptional activity by use of the specific HIF-2a inhibitor PT2385 abolished all effects of DLK1 on stem cell marker gene expression and colony formation under hypoxic conditions. Interestingly, DLK1 expression itself has been shown to be regulated by hypoxia in other cell systems [19,20], suggesting that there may be a DLK1-HIF feedback loop in hypoxic tumor cells. In the present investigation, effects of DLK1 treatment were enhanced by hypoxic culture conditions. Importantly, however, HIF-2a inhibition did not significantly affect DLK1-mediated stem cell marker expression under normoxic conditions, suggesting that there are other mediators downstream of DLK1 that can contribute to DLK1 signaling in glioma.

Several questions remain regarding signaling mediated by soluble DLK1, including that of potential receptors for DLK1. Among the human glioma cell lines and genetically engineered glioma mouse model tested in this study, all but one cell line (U3065MG) responded to soluble DLK1. Based on the experiments presented here, it is difficult to determine the reason for the lack of response in this cell line. It is possible that U3065MG cells lack expression of necessary components downstream of soluble DLK1. Further investigation into potential receptors and downstream mediators of DLK1 signaling is warranted, to better infer the applicability of the DLK1-mediated effects described in this study. Furthermore, it is somewhat counterintuitive that soluble DLK1 appears to simultaneously promote glioma cell proliferation and stem cell characteristics, as it is widely assumed that stem-like cells display lower proliferation rates than more differentiated, non–stem-like cells.

Conclusions

Taken together, our data support a role for soluble DLK1 as a tumor-promoting stem cell niche factor in glioma. Further research is warranted to investigate whether or not signaling by DLK1 can be therapeutically targeted, either via HIF2-a inhibition or by targeting upstream signaling.

Acknowledgments

The authors thank Christina Möller for technical assistance and A Human Glioblastoma Cell Culture Resource (www.hgcc.se) (Lene Uhrbom, Bengt Westermark, Karin Forsberg Nilsson and Sven Nelander, Uppsala University, Sweden) for human GBM cultures.

Authors' Contributions

ESG: Conceptualization; Data curation; Formal analysis; Investigation; Methodology; Validation; Visualization; Roles/Writing – original draft; Writing – review & editing. PJ: Formal analysis; Investigation; Methodology; Validation; Visualization; Writing – review & editing. VP: Formal analysis Investigation; Methodology; Validation; Visualization; Writing – review & editing. TJB: Formal analysis; Investigation; Methodology; Validation; Visualization; Writing – review & editing. AP: Conceptualization; Data

curation; Formal analysis; Funding acquisition; Project administration; Resources; Supervision; Roles/Writing – original draft; Writing – review & editing.

Supplementary materials

Supplementary material associated with this article can be found, in the online version, at doi:10.1016/j.neo.2020.10.005.

References

[1] Huse JT, Holland EC. Targeting brain cancer: advances in the molecular pathology of malignant glioma and medulloblastoma. *Nat Rev Cancer* 2010;**10**(5):319–31. doi:10.1038/nrc2818.

[2] Bernstock JD, Mooney JH, Ilyas A, Chagoya G, Estevez-Ordonez D, Ibrahim A, Nakano I. Molecular and cellular intratumoral heterogeneity in primary glioblastoma: clinical and translational implications. *J Neurosurg* 2019:1–9. doi:10.3171/2019.5.JNS19364.

[3] Dirkse A, Golebiewska A, Buder T, Nazarov PV, Muller A, Poovathingal S, Niclou SP. Stem cell-associated heterogeneity in Glioblastoma results from intrinsic tumor plasticity shaped by the microenvironment. *Nat Commun* 2019;**10**(1):1787. doi:10.1038/s41467-019-09853-z.

[4] Hambardzumyan D, Bergers G. Glioblastoma: defining tumor niches. *Trends Cancer* 2015;**1**(4):252–65. doi:10.1016/j.trecan.2015.10.009.

[5] Jawhari S, Ratinaud M-H, Verdier M. Glioblastoma, hypoxia and autophagy: a survival-prone "ménage-à-trois". *Cell Death Dis* 2016;**7**(10):e2434. doi:10.1038/cddis.2016.318.

[6] Ryskalin L, Gaglione A, Limanaqi F, Biagioni F, Familiari P, Frati A, Fornai F. The autophagy status of cancer stem cells in gliobastoma multiforme: from cancer promotion to therapeutic strategies. *Int J Mol Sci* 2019 MDPI AG. doi:10.3390/ijms20153824.

[7] Majmundar AJ, Wong WJ, Simon MC. Hypoxia-inducible factors and the response to hypoxic stress. *Mol Cell* 2010;**40**(2):294–309. doi:10.1016/j.molcel.2010.09.022.

[8] Baladrón V, Ruiz-Hidalgo MJ, Nueda ML, Díaz-Guerra MJM, García-Ramírez JJ, Bonvini E, Laborda J. dlk acts as a negative regulator of Notch1 activation through interactions with specific EGF-like repeats. *Exp Cell Res* 2005;**303**(2):343–59. doi:10.1016/j.yexcr.2004.10.001.

[9] Ceder JA, Jansson L, Helczynski L, Abrahamsson P-A. Delta-like 1 (Dlk-1), a novel marker of prostate basal and candidate epithelial stem cells, is downregulated by notch signalling in intermediate/transit amplifying cells of the human prostate. *Eur Urol* 2008;**54**(6):1344–53. doi:10.1016/j.eururo.2008.03.006.

[10] Falix FA, Aronson DC, Lamers WH, Gaemers IC. Possible roles of DLK1 in the Notch pathway during development and disease. *Biochim Biophys Acta* 2012;**1822**(6):988–95. doi:10.1016/j.bbadis.2012.02.003.

[11] Ferrón SR, Charalambous M, Radford E, McEwen K, Wildner H, Hind E, Ferguson-Smith AC. Postnatal loss of Dlk1 imprinting in stem cells and niche astrocytes regulates neurogenesis. *Nature* 2011;**475**(7356):381–5. doi:10.1038/nature10229.

[12] Huang C-C, Cheng S-H, Wu C-H, Li W-Y, Wang J-S, Kung M-L, Tai M-H. Delta-like 1 homologue promotes tumorigenesis and epithelial-mesenchymal transition of ovarian high-grade serous carcinoma through activation of Notch signaling. *Oncogene* 2019;**38**(17):3201–15. doi:10.1038/s41388-018-0658-5.

[13] Li L, Tan J, Zhang Y, Han N, Di X, Xiao T, Liu Y. DLK1 promotes lung cancer cell invasion through upregulation of MMP9 expression depending on Notch signaling. *PLoS One* 2014;**9**(3):e91509. doi:10.1371/journal.pone.0091509.

[14] Grassi ES, Pantazopoulou V, Pietras A. Hypoxia-induced release, nuclear translocation, and signaling activity of a DLK1 intracellular fragment in glioma. *Oncogene* 2020:1–17. doi:10.1038/s41388-020-1273-9.

[15] Yin D, Xie D, Sakajiri S, Miller CW, Zhu H, Popoviciu ML, Koeffler HP. DLK1: increased expression in gliomas and associated with oncogenic activities. *Oncogene* 2006;**25**(13):1852–61. doi:10.1038/sj.onc.1209219.

[16] Wang Y, Sul HS. Ectodomain shedding of preadipocyte factor 1 (Pref-1) by tumor necrosis factor alpha converting enzyme (TACE) and inhibition of adipocyte differentiation. *Mol Cell Biol* 2006;**26**(14):5421–35. doi:10.1128/MCB.02437-05.

[17] Mega A, Hartmark Nilsen M, Leiss LW, Tobin NP, Miletic H, Sleire L, Östman A. Astrocytes enhance glioblastoma growth. *Glia* 2020;**68**(2):316–27. doi:10.1002/glia.23718.

[18] Katz AM, Amankulor NM, Pitter K, Helmy K, Squatrito M, Holland EC. Astrocyte-specific expression patterns associated with the PDGF-induced glioma microenvironment. *PLoS One* 2012;**7**(2):e32453. doi:10.1371/journal.pone.0032453.

[19] Begum A, Kim Y, Lin Q, Yun Z. DLK1, delta-like 1 homolog (Drosophila), regulates tumor cell differentiation in vivo. *Cancer Lett* 2012;**318**(1):26–33. doi:10.1016/j.canlet.2011.11.032.

[20] Kim Y, Lin Q, Zelterman D, Yun Z. Hypoxia-regulated delta-like 1 homologue enhances cancer cell stemness and tumorigenicity. *Cancer Res* 2009;**69**(24):9271–80. doi:10.1158/0008-5472.CAN-09-1605.

[21] Holland EC, Hively WP, DePinho RA, Varmus HE. A constitutively active epidermal growth factor receptor cooperates with disruption of G1 cell-cycle arrest pathways to induce glioma-like lesions in mice. *Genes Dev* 1998;**12**(23):3675–85. doi:10.1101/gad.12.23.3675.

[22] Ozawa T, Riester M, Cheng YK, Huse JT, Squatrito M, Helmy K, Charles N, Michor F, Holland EC. Most human non-GCIMP glioblastoma subtypes evolve from a common proneural-like precursor glioma. *Cancer Cell* 2014;**26**(2):288–300. doi:10.1016/j.ccr.2014.06.005.

[23] Johansson E, Grassi ES, Pantazopoulou V, Tong B, Lindgren D, Berg TJ, Pietras A. CD44 Interacts with HIF-2α to modulate the hypoxic phenotype of perinecrotic and perivascular glioma cells. *Cell Rep* 2017;**20**(7). doi:10.1016/j.celrep.2017.07.049.

[24] Xie Y, Bergström T, Jiang Y, Johansson P, Marinescu VD, Lindberg N, Uhrbom L. The human glioblastoma cell culture resource: validated cell models representing all molecular subtypes. *EBioMedicine* 2015;**2**(10):1351–63. doi:10.1016/j.ebiom.2015.08.026.

[25] Sun Y, Vandenbriele C, Kauskot A, Verhamme P, Hoylaerts MF, Wright GJ A human platelet receptor protein microarray identifies FcepsilonR1alpha as an activating PEAR1 ligand. *Mol Cell Proteomics* 2015. doi:10.1074/mcp.M114.046946.

[26] Emerling BM, Weinberg F, Liu J-L, Mak TW, Chandel NS. PTEN regulates p300-dependent hypoxia-inducible factor 1 transcriptional activity through Forkhead transcription factor 3a (FOXO3a). *Proc Natl Acad Sci USA* 2008;**105**(7):2622–7. doi:10.1073/pnas.0706790105.

[27] Ceccarelli M, Barthel FP, Malta TM, Sabedot TS, Salama SR, Murray BA, Verhaak RGW. Molecular profiling reveals biologically discrete subsets and pathways of progression in diffuse glioma. *Cell* 2016;**164**(3):550–63. doi:10.1016/j.cell.2015.12.028.

[28] Zhao Z, Zhang K, Wang Q, Li G, Zeng F, Zhang Y, et al. Chinese glioma genome atlas (CGGA): a comprehensive resource with functional genomic data for Chinese glioma patients. 2020. bioRxiv. Cold Spring Harbor Laboratory; 2020.01.20.911982. doi:10.1101/2020.01.20.911982.

[29] Bowman RL, Wang Q, Carro A, Verhaak RGW, Squatrito M. GlioVis data portal for visualization and analysis of brain tumor expression datasets. *Neuro Oncol* 2017;**19**(1):139–41. doi:10.1093/neuonc/now247.

[30] Jensen RL. Brain tumor hypoxia: tumorigenesis, angiogenesis, imaging, pseudoprogression, and as a therapeutic target. *Journal of Neuro-Oncology*. Kluwer Academic Publishers; 2009. doi:10.1007/s11060-009-9827-2.

[31] Das B, Pal B, Bhuyan R, Li H, Sarma A, Gayan S, Felsher DW. MYC regulates the HIF2α stemness pathway via Nanog and Sox2 to maintain self-renewal in cancer stem cells versus non-stem cancer cells. *Cancer Res* 2019;**79**(16):4015–25. doi:10.1158/0008-5472.CAN-18-2847.

[32] Pietras A, Gisselsson D, Ora I, Noguera R, Beckman S, Navarro S, Påhlman S. High levels of HIF-2alpha highlight an immature neural crest-like neuroblastoma cell cohort located in a perivascular niche. *J Pathol* 2008;**214**(4):482–8. doi:10.1002/path.2304.

[33] Pietras A, Johnsson AS, Påhlman S. The HIF-2α-driven pseudo-hypoxic phenotype in tumor aggressiveness, differentiation, and

vascularization. *Curr Top Microbiol Immunol* 2010;**345**:1–20. doi:10.1007/82_2010_72.

[34] Yan Y, Liu F, Han L, Zhao L, Chen J, Olopade OI, Wei M. HIF-2α promotes conversion to a stem cell phenotype and induces chemoresistance in breast cancer cells by activating Wnt and Notch pathways. *J Exp Clin Cancer Res* 2018;**37**(1):256. doi:10.1186/s13046-018-0925-x.

[35] Persson CU, von Stedingk K, Fredlund E, Bexell D, Påhlman S, Wigerup C, Mohlin S. ARNT-dependent HIF-2 transcriptional activity is not sufficient to regulate downstream target genes in neuroblastoma. *Exp Cell Res* 2020;**388**(2):111845. doi:10.1016/j.yexcr.2020.111845.

[36] Wallace EM, Rizzi JP, Han G, Wehn PM, Cao Z, Du X, Josey JA. A small-molecule antagonist of HIF2α is efficacious in preclinical models of renal cell carcinoma. *Cancer Res* 2016;**76**(18):5491–500. doi:10.1158/0008-5472.CAN-16-0473.

[37] Dirks PB. Brain tumor stem cells: the cancer stem cell hypothesis writ large. *Molecular Oncology*. John Wiley and Sons Ltd; 2010. doi:10.1016/j.molonc.2010.08.001.

[38] Lathia JD, Mack SC, Mulkearns-Hubert EE, Valentim CLL, Rich JN. Cancer stem cells in glioblastoma. *Genes and Development*. Cold Spring Harbor Laboratory Press; 2015. doi:10.1101/gad.261982.115.

[39] Hira VVV, Breznik B, Vittori M, Loncq de Jong A, Mlakar J, Oostra RJ, Khurshed M, Molenaar RJ, Lah T, Van Noorden CJF. Similarities between stem cell niches in glioblastoma and bone marrow: rays of hope for novel treatment strategies. *J Histochem Cytochem* 2020;**68**(1):33–57. doi:10.1369/0022155419878416.